Performance Bounds for a Maxima-Sampling Envelope Detector [Full Equation Derivations]

Swagat Bhattacharyya

I. Introduction

THIS document provides full derivations and assumptions for the formulae in corresponding peer-reviewed work titled "Performance Bounds for a Maxima-Sampling Envelope Detector." Maxima-sampling envelope detectors (MSEDs) demodulate by peak sampling, avoiding the latency–ripple trade-off in conventional non-sampled envelope detectors [1]. Avoiding the latency-ripple tradeoff is highly beneficial to applications such as design of stable AGC loops across wide frequency ranges [2]. However, MSEDs lack a rigorous analytical foundation, with prior designs relying on empirical methods.

Fundamentally, MSEDs operate by nonuniformly sampling at half the local carrier frequency, using aliasing for demodulation. This process also introduces aliasing artifacts; thus, performance depends on the ratio of desired to undesired aliasing, which in turn depends on input characteristics. Designers need clear performance guarantees to adopt MSEDs.

This work derives and validates performance bounds for MSEDs based on time- and frequency-domain properties. Key insights include the role of modulation rate relative to carrier frequency and design rules for practical use. Contributions are:

- A unified analytical framework for generic envelope signals.
- Tight bounds for specific envelope signal types.

Note that a red box around an equation in a display math environment indicates that the equation was presented in the corresponding peer-review work.

II. Frequency-Domain Intuition

Undesired aliasing, which occurs in the presence of any amplitude-modulated input, limits MSED performance. Let us first consider the unitless finite-energy test signal $V_{in}(t) = \cos(\omega_0 t)\exp(-at)\Theta(t)$, where $a > 0$, and $\Theta(t)$ denotes the unit step (Fig. 1(a)). This V_{in} arises as the natural response of an underdamped second-order system with quality factor $Q = \omega_0/2a$ and approximates the local behavior of many electronic oscillators. Aliasing can be studied by modeling a MSED as an impulse-train sampler clocked at ω_0 followed by a zero-order hold [2]. The output spectrum is then:

$$V_{out}(j\omega) = \left[\frac{1}{2\pi}\left\{\omega_0 \sum_{k=-\infty}^{\infty} \delta\left(\omega - k\omega_0\right)\right\} * \left\{V_{in}\left(j\omega\right)\right\}\right] \cdot \left[2\sin\left(\frac{\pi\omega}{\omega_0}\right)\exp\left(-\frac{j\pi\omega}{\omega_0}\right)\Big/\omega\right] \rightarrow \tag{1}$$

$$V_{out}(j\omega) = \left[\frac{\omega_0}{2\pi}\sum_{k=-\infty}^{\infty} V_{in}\left(\omega - k\omega_0\right)\right] \cdot \left[2\sin\left(\frac{\pi\omega}{\omega_0}\right)\exp\left(-\frac{j\pi\omega}{\omega_0}\right)\Big/\omega\right] \rightarrow \tag{2}$$

$$V_{out}(j\omega) = \frac{\omega_0}{4\pi}\left[\sum_{k=-\infty}^{\infty}\frac{1}{a + j\left(\omega - k\omega_0 - \omega_0\right)} + \sum_{k=-\infty}^{\infty}\frac{1}{a + j\left(\omega - k\omega_0 + \omega_0\right)}\right] \cdot \left[2\sin\left(\frac{\pi\omega}{\omega_0}\right)\exp\left(-\frac{j\pi\omega}{\omega_0}\right)\Big/\omega\right] \rightarrow \tag{3}$$

$$\boxed{V_{out}(j\omega) = \sum_{k=-\infty}^{\infty}\left(\frac{\exp\left(-\frac{j\pi\omega}{\omega_0}\right)}{a + j(\omega - k\omega_0)} \cdot \frac{\sin\left(\frac{\pi\omega}{\omega_0}\right)}{\frac{\pi\omega}{\omega_0}}\right)} \tag{4}$$

At low Q, $V_{out}(j\omega)$ is quite distorted, while at high Q, $V_{out}(j\omega)$ approaches the spectrum of the modulation signal. While useful for visualization, this frequency-domain representation is not amenable to quantifying aliasing extent, as each summand

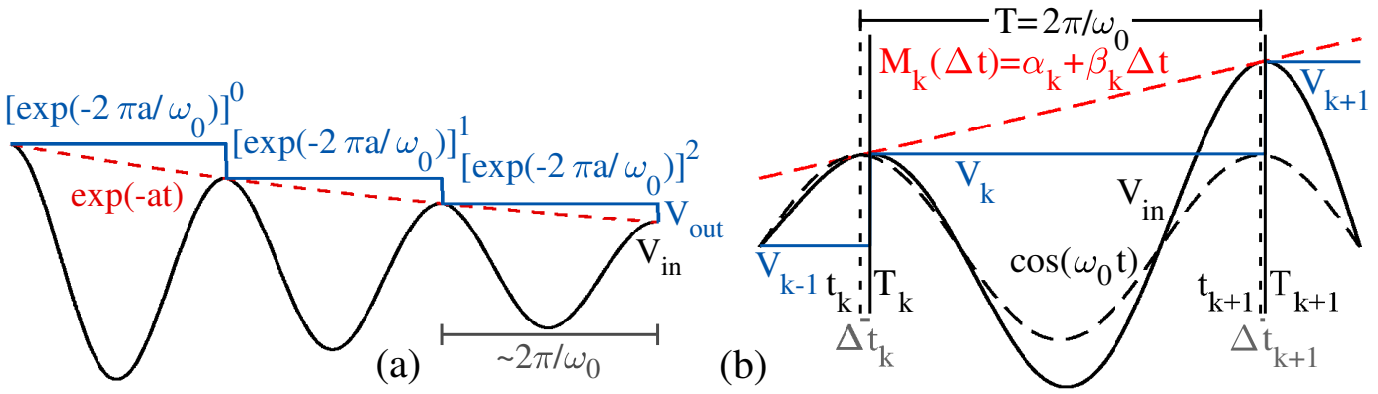

Fig. 1. (a) Annotated MSED input (V_{in}) and output (V_{out}) corresponding to Section II derivations. (b) Geometric basis of the time-domain analyses in Section III, where the modulation signal is approximated piecewise via line segments with endpoints at carrier signal maxima.

in Eq. 4 has infinite spectral support. To quantify the severity of undesired aliasing, we define U: the ratio of the demodulation error signal energy to the modulation signal energy. We compute U through a time-domain approach:

$$\boxed{U = \int_0^\infty |V_{out}(t) - \exp(-at)|^2 dt \Big/ \int_0^\infty |\exp(-at)|^2 dt} = 2a \int_0^\infty |V_{out}(t) - \exp(-at)|^2 dt =$$
$$2a \sum_{k=0}^{\infty} \int_{2\pi k/\omega_0}^{2\pi(k+1)/\omega_0} \left| V_{out}\left(\frac{2\pi k}{\omega_0}\right) - \exp(-at) \right|^2 dt \approx 2a \sum_{k=0}^{\infty} \int_{2\pi k/\omega_0}^{2\pi(k+1)/\omega_0} |\exp(-\pi k/Q) - \exp(-at)|^2 \, dt \quad (Q \gg 1) =$$
$$2a \sum_{k=0}^{\infty} \int_0^{2\pi/\omega_0} |\exp(-\pi k/Q) - \exp(-a\,(\tau + 2\pi k/\omega_0))|^2 \, d\tau = \boxed{2a \sum_{k=0}^{\infty} \exp\left(-\frac{2\pi k}{Q}\right) \int_0^{2\pi/\omega_0} [1 - \exp(-a\tau)]^2 \, d\tau} =$$
$$\frac{2a\left[\frac{2\pi}{\omega_0} + \frac{2}{a}\left(\exp\left(-\frac{2\pi a}{\omega_0}\right) - 1\right) - \frac{1}{2a}\left(\exp\left(-\frac{4\pi a}{\omega_0}\right) - 1\right)\right]}{1 - \exp\left(-2\pi/Q\right)} = \boxed{\frac{4\exp(-\pi/Q) - \exp(-2\pi/Q) + 2\pi/Q - 3}{1 - \exp(-2\pi/Q)}}. \tag{5}$$

Eq. 5 shows that there is a steep trade-off between Q and undesired aliasing severity U. Note that at low Q, a key assumption underlying Eq. 5 (i.e., negligible perturbation in maxima locations) is not valid, and at high Q, numerical simulation accuracy suffers from numerical integration error. The analyses thus far imply that the input envelope should vary minimally within the span of a carrier period to yield an undistorted envelope estimate.

However, extending the cumbersome analytical methods in this section is neither straightforward nor necessary for most applications. In any case, we must also relax the implicit assumption of pseudo-uniform sampling, as maxima sampling is inherently nonuniform. We propose the use of time-domain analysis based on a piecewise linearization of the modulation signal as a means to address the poor complexity scaling of the previous methods. As a preview of its efficacy, we can evaluate the prediction of the linearization method (found by substituting $P_k = 1/2Q$ into Eq. 20 and keeping the first two terms):

$$\boxed{U \sim 1/3Q^2 + \pi/8Q^3.} \tag{6}$$

Eq. 6 is tight for high Q, where the modulation signal varies slowly relative to the carrier; Eq. 6 is not tight at low Q due to the invalid assumption of negligible higher-order terms in the expansion of the modulation signal.

III. Piecewise Time-Domain Analysis

Let us consider a real-valued amplitude-modulated MSED input of form: $V_{in}(t) = M(t)\cos(\omega_0 t)$, where $M(t) > 0$ ($\forall t \in \mathbb{R}$), which ensures nonzero input signal energy over any carrier period and no inversion in the relative carrier phase. The geometry underlying our piecewise analysis is shown in Fig. 1(b), and the approach taken is as follows: (1) find the maxima timestamp perturbation (Δt_k) due to modulation, (2) find integration bounds and maxima values (V_k) from Δt_k, (3) estimate the local undesired aliasing severity U_k based on V_k and Δt_k, and (4) show how to estimate U_k for a test signal.

A. Estimation of Maxima Timestamps

We start our estimation of input maxima timestamps by enforcing the first derivative constraint on $V_{in}(t)$:

$$\dot{V}_{in}(t) = \dot{M}(t)\cos(\omega_0 t) - \omega_0 M(t)\sin(\omega_0 t) = 0 \rightarrow \boxed{\dot{M}(t)/M(t) = \omega_0 \tan(\omega_0 t)\,.} \tag{7}$$

We assume $M(t)$ can be linearized everywhere; a sufficient condition for a linearization to exist is that $M(t)$ be bandlimited to some bandwidth Ω—in which case the Paley-Wiener Theorem [3] assures that $M(t)$ is in C^{∞}. We denote the linearization of $M(t)$ about the k$^{\text{th}}$ maximum of the carrier signal as: $M_k(\Delta t) := \alpha_k + \beta_k \Delta t$. The maxima of the carrier signal $\cos(\omega_0 t)$ occur at $t_k = Tk = 2\pi k/\omega_0$ ($\forall k \in \mathbb{Z}$), and the perturbation of the maxima timestamps due to modulation (denoted $\Delta t_k := T_k - t_k$) can be estimated by invoking the small-angle approximation on Eq. 7:

$$\boxed{\frac{\beta_k/\omega_0^2}{\alpha_k + \beta_k \Delta t_k} \approx \Delta t_k} \rightarrow \omega_0^2 \beta_k \left(\Delta t_k\right)^2 + \omega_0^2 \alpha_k \left(\Delta t_k\right) - \beta_k \approx 0 \rightarrow \boxed{\Delta t_k \approx -\frac{\alpha_k}{2\beta_k} + \frac{\sqrt{\omega_0^2 \alpha_k^2 + 4\beta_k^2}}{2\omega_0 \beta_k}}. \tag{8}$$

Expanding Eq. 8 further is helpful in further analysis. To keep equation "entropy" under control, we invoke the intuition built in Section II, which found only the *relative* rate of change between the modulating and carrier signal to be of importance. Thus, normalizing timescales to the carrier period simplifies analysis. To this end, we define:

$$\boxed{P_k := \frac{M_k\left(T\right) - M_k\left(0\right)}{M_k(0)} = \frac{\beta_k T}{\alpha_k} = \frac{2\pi\beta_k}{\alpha_k \omega_0};\ \mathcal{P}_k := \frac{P_k}{2\pi}}, \tag{9}$$

where P_k represents the 'Percent' increase in $M(t)$ between carrier maxima, and $\mathcal{P}_k := P_k/2\pi$ is defined for convenience. We now expand the square root in Eq. 8 about $\beta_k = 0$:

$$\begin{gathered}\boxed{\sqrt{\omega_0^2 \alpha_k^2 + 4\beta_k^2} = \sum_{n=0}^{\infty} \left[\left(4\beta_k^2\right)^n \left(\omega_0^2 \alpha_k^2\right)^{\frac{1}{2}-n} \binom{1/2}{n}\right]} \quad \left(4\beta_k^2 < \omega^2 \alpha_k^2\right) = \\ \alpha_k \omega_0 \sum_{n=0}^{\infty} \left[\frac{\left(4\beta_k^2\right)^n}{\left(\omega_0^2 \alpha_k^2\right)^n} \cdot \binom{2n}{n} \cdot \frac{(-1)^{n+1}}{2^{2n}\left(2n-1\right)}\right] \quad (\alpha_k > 0) = \boxed{\alpha_k \omega_0 \textstyle\sum_{n=0}^{\infty} \left[\zeta_n \mathcal{P}_k^{2n}\right];\ \ \zeta_n = \frac{(-1)^{n+1}\left(2n\right)!}{\left(2n-1\right)\left(n!\right)^2}}\end{gathered} \tag{10}$$

where the region of convergence condition for the series simplifies to $\left|\mathcal{P}_k\right| < 1/2$. We now isolate Δt_k by substituting Eq. 10 into Eq. 8 and simplifying:

$$\Delta t_k \approx -\frac{\alpha_k}{2\beta_k} + \frac{\alpha_k}{2\beta_k} \sum_{n=0}^{\infty} \left[\zeta_n \mathcal{P}_k^{2n}\right] \xrightarrow[\frac{\zeta_n}{\zeta_{n-1}} = \frac{6-4n}{n}]{\zeta_0 = 1,\ \frac{\alpha_k}{2\beta_k} = \frac{\mathcal{P}_k^{-1}}{2\omega_0}} \boxed{\Delta t_k \approx \sum_{n=1}^{\infty} \left[\frac{\zeta_n \mathcal{P}_k^{2n-1}}{2\omega_0}\right];\ \ \zeta_n = \begin{cases} \frac{6-4n}{n}\zeta_{n-1}, & n > 1 \\ 2, & n = 1 \end{cases}}. \tag{11}$$

Agreement between theory and numerical simulation is excellent when $\mathcal{P}_k < 1/2\pi$, which makes the small-angle approximation used for Eq. 8 valid. When $\mathcal{P}_k < 1/2\pi$, the first-order term suffices for most computations since its magnitude tightly bounds the value of $|\Delta t_k|$ (due to the alternating signs and rapidly decaying magnitude of subsequent terms). To first order, the timestamp of the k$^{\text{th}}$ peak of $V_{in}(t)$ is:

$$\boxed{T_k = t_k + \Delta t_k \approx \left(2\pi k + \mathcal{P}_k\right)/\omega_0; \quad \left(\mathcal{P}_k < 1/2\pi\right).} \tag{12}$$

B. Piecewise Analytic Estimation of Undesired Aliasing

We estimate the undesired aliasing severity between the k$^{\text{th}}$ and (k+1)$^{\text{th}}$ peak (U_k) by normalizing the demodulation error:

$$\boxed{U_k := \frac{\frac{1}{T}\int_{\Delta t_k}^{T+\Delta t_{k+1}} \left[V_k - M_k(t)\right]^2 dt}{\frac{1}{T}\int_{\Delta t_k}^{T+\Delta t_{k+1}} M_k(t)^2 dt}}. \tag{13}$$

We first solve for an intermediate quantity for convenience by using Eq. 11:

$$T + \Delta t_{k+1} - \Delta t_k = T + \frac{1}{\omega_0}\left[\left(\mathcal{P}_{k+1} - \mathcal{P}_{k+1}^3 + \mathcal{O}\left(\mathcal{P}_{k+1}^5\right)\right) - \left(\mathcal{P}_k - \mathcal{P}_k^3 + \mathcal{O}\left(\mathcal{P}_k^5\right)\right)\right], \text{ where} \tag{14}$$

$$\mathcal{P}_{k+1} \approx \frac{\beta_k T}{2\pi\alpha_{k+1}} = \frac{\beta_k T}{2\pi\left(\alpha_k + \beta_k T\right)} = \frac{\mathcal{P}_k}{1 + 2\pi\mathcal{P}_k}, \tag{15}$$

assuming that $\beta_{k+1} = \beta_k$ (i.e., that $\ddot{M}(t)$ is negligible). Then, substituting Eq. 15 into Eq. 14:

$$\begin{gathered}T + \Delta t_{k+1} - \Delta t_k = T + \frac{1}{\omega_0}\left[\left(\frac{\mathcal{P}_k}{1+2\pi\mathcal{P}_k} - \mathcal{P}_k\right) + \mathcal{O}\left(\frac{\mathcal{P}_k^4}{\left(1+2\pi\mathcal{P}_k\right)^3}\right)\right] = \\ T\left[1 - \frac{\mathcal{P}_k^2}{1+2\pi\mathcal{P}_k} + \mathcal{O}\left(\frac{\mathcal{P}_k^4}{\left(1+2\pi\mathcal{P}_k\right)^3}\right)\right] \approx T\left(1 - \mathcal{P}_k^2\right) \quad \left(\mathcal{P}_k \ll 1\right)\end{gathered} \tag{16}$$

Now, we can solve for the denominator of Eq. 13:

$$\frac{1}{T}\int_{\Delta t_k}^{T+\Delta t_{k+1}} M_k(t)^2 dt = \frac{1}{T}\int_{0}^{T+\Delta t_{k+1}-\Delta t_k} M_k(\tau+\Delta t_k)^2 d\tau = \frac{1}{T}\int_{0}^{T\left(1-P_k^2\right)} \left[\alpha_k+\beta_k(\tau+\Delta t_k)\right]^2 d\tau =$$

$$\frac{\alpha_k^2}{T}\int_{0}^{T\left(1-P_k^2\right)} \left[\left(1+\frac{\beta_k \Delta t_k}{\alpha_k}\right)+\frac{\beta_k \tau}{\alpha_k}\right]^2 d\tau \xrightarrow[P_k=\frac{\beta_k}{\alpha_k\omega_0}]{\Delta t_k=\frac{P_k-P_k^3+2P_k^5+\mathcal{O}\left(P_k^7\right)}{\omega_0}} \tag{17}$$

$$\frac{\alpha_k^2}{T}\int_{0}^{T\left(1-P_k^2\right)} \left[\left(1+P_k^2-P_k^4+2P_k^6+\mathcal{O}\left(P_k^8\right)\right)+\frac{2\pi P_k}{T}\tau\right]^2 d\tau = \alpha_k^2\left(1+2\pi P_k+\mathcal{O}\left(P_k^2\right)\right).$$

Now, the MSED hold level (V_k) follows by inserting Δt_k (Eq. 11) into a parabolic approximation of V_{in}: $V_k = \alpha_k + \beta_k \Delta t_k - \alpha_k \omega_0^2 \Delta t_k^2/2 + \mathcal{O}\left(\Delta t_k^3\right)$. Substituting V_k and Eq. 17 into Eq. 13 yields:

$$U_k \approx \frac{\frac{1}{T}\int_{\Delta t_k}^{T+\Delta t_{k+1}} \left[\left(\alpha_k+\beta_k\Delta t_k-\frac{\alpha_k\omega_0^2\Delta_k^2}{2}+\mathcal{O}\left(\Delta t_k^3\right)\right)-\left(\alpha_k+\beta_k t\right)\right]^2 dt}{\alpha_k^2\left(1+2\pi P_k+\mathcal{O}\left(P_k^2\right)\right)} =$$

$$\boxed{\frac{\int_0^{T(1-P_k^2)}\left[\beta_k\tau+\alpha_k\omega_0^2\Delta t_k^2/2+\mathcal{O}\left(\Delta t_k^3\right)\right]^2 d\tau}{T\alpha_k^2\left(1+2\pi P_k+\mathcal{O}\left(P_k^2\right)\right)}} = \boxed{\frac{4\pi^2\beta_k^2/3\omega_0^2+\pi\beta_k\alpha_k\omega_0\Delta t_k^2+\mathcal{O}\left(\Delta t_k^3\right)}{\alpha_k^2\left(1+2\pi P_k+\mathcal{O}\left(P_k^2\right)\right)}} \tag{18}$$

By substituting Eq. 11 into Eq. 18 and simplifying:

$$U_k \approx \frac{\frac{4\pi^2P_k^2}{3}\left[1-2P_k^2+\frac{3P_k\left(1-P_k^2\right)^3}{4\pi}+\frac{3\pi^2P_k^2\left(1-P_k^2\right)^4}{(2\pi)^4}\right]}{1+2\pi P_k+\mathcal{O}\left(P_k^2\right)} = \frac{4\pi^2P_k^2/3+\pi P_k^3+\left(1/4-8\pi^2/3\right)P_k^4+\mathcal{O}\left(P_k^5\right)}{1+2\pi P_k+\mathcal{O}\left(P_k^2\right)} \tag{19}$$

$$\rightarrow \boxed{U_k \approx 4\pi^2P_k^2/3+\pi P_k^3+\left(1/4-8\pi^2/3\right)P_k^4+\mathcal{O}\left(P_k^5\right)} \quad \left(|P_k| \ll 1/2\pi\right) \tag{20}$$

When $|P_k| \ll 1/2\pi$, a second-order truncation of Eq. 20 already closely follows numerical simulations. For low P_k, U_k grows by 20 dB per decade of P_k; U_k growth rate tapers for large P_k.

C. Example: Estimated Bound for Sinusoidal Modulation

Sinusoidal modulation is interesting to study because output amplitude may itself oscillate in poorly tuned oscillator AGC loops. In such cases, amplitude modulation index is usually limited by higher-order nonlinearities [4]. Without loss of generality, let V_{in} be modulated at rate ω_m with modulation index m, where $0 \le m < 1$ to avoid phase reversal:

$$\boxed{V_{in}(t) = \left(1+m\cdot\cos\left(\omega_0 w t\right)\right)\cos\left(\omega_0 t\right),} \tag{21}$$

where $w := \omega_m/\omega_0$. Substituting Eq. 21 into Eq. 9 yields:

$$\boxed{P_k = -w\cdot\sin\left(2\pi k w\right)/\left(\cos\left(2\pi k w\right)+1/m\right).} \tag{22}$$

By observing the odd parity of Eq. 22, it is easy to prove by contradiction that $\max P_k = -\min P_k$. So:

$$\boxed{\left|P_k\right| \le w\cdot\max_{x\in[0,\pi]}\frac{\sin x}{\cos x+1/m} = w\cdot m/\sqrt{1-m^2},} \tag{23}$$

where the final expression is obtained by enforcing a zero derivative condition on the operand of the 'max' function:

$$\cos(x)\left(\frac{1}{m}+\cos(x)\right)+\sin^2(x)=0 \rightarrow \frac{1}{m}\cos(x)+1=0 \rightarrow \begin{cases}\cos(x)=-m\\ \sin(x)=\sqrt{1-m^2}\end{cases} \tag{24}$$

Eq. 23 is valid when $\left|P_k\right| \ll 1/2\pi$ due to the limitations of the linearization approach in capturing the perturbation in maxima locations; we also require $m < 1$. Substituting Eq. 23 into Eq. 23 yields:

$$\max\left(U_k\right) = \left(4\pi^2/3\right)w^2m^2/\left(1-m^2\right)+\pi w^3m^3/\left(1-m^2\right)^{3/2}+\mathcal{O}\left(w^4m^4/\left(1-m^2\right)^2\right) \tag{25}$$

$$\boxed{\text{Hence: } \max\left(U_k\right) \approx \left(4\pi^2/3\right)w^2m^2/\left(1-m^2\right).} \tag{26}$$

At low w and m, Eq. 26 clearly shows that U_k asymptotically rises by 20 dB/dec relative to m; $\max\left(U_k\right)$ spikes when $m > 0.5$.

IV. Bound by Marriage of Time and Frequency

While previous bounds are tight in their stated regimes, circuit designers usually know only a few time- and frequency-domain properties of V_{in} apriori: carrier rate (ω_0), amplitude modulation index (m), and modulation signal bandwidth (Ω). We thus reformulate the bound on U_k using only these three properties. Without loss of generality, let: $M(t) = 1 + m \cdot \widetilde{M}(t)$, where $\widetilde{M}(t) \in [-1, 1]$ is bandlimited to Ω, and $0 \leq m < 1$ to avoid phase reversal. The key step in our derivation is to bound $|P_k|$, which depends on $|\dot{M}(t)/M(t)|$. The tight Bernstein inequality [5] states that for any $f(t)$ bandlimited to Ω:

$$\boxed{|\dot{f}(t)| \leq \Omega \cdot \sup_{t\in\mathbb{R}}|f(t)|.} \tag{27}$$

We can substitute $f(t) = \ln(M(t))$ into Eq. 27 to get:

$$\boxed{|P_k| = \frac{1}{\omega_0}\left|\frac{\dot{M}}{M}\right| \leq W \cdot \sup_{t\in\mathbb{R}}|\ln M| = -W \cdot \ln(1-m),} \tag{28}$$

where $W := \Omega/\omega_0$. Substituting Eq. 28 into Eq. 20 yields:

$$\max(U_k) = \left(4\pi^2/3\right) W^2 \ln^2(1-m) - \pi W^3 \ln^3(1-m) + \mathcal{O}\left(W^4 \ln^4(1-m)\right) \rightarrow \tag{29}$$

$$\boxed{\max(U_k) \approx \left(4\pi^2/3\right) W^2 \ln^2(1-m),} \tag{30}$$

for $\max(U_k) < 1/3$. The bound in Eq. 30 holds well when $\max(U_k) < 1/3$ and becomes tighter for large m and small W. $\max(U_k)$ increases by 2 dec/dec relative to both the normalized bandwidth and the modulation index at low m and that V_{in} should have $m \ll 0.5$ for accurate MSED tracking.

References

[1] J. Alegre, S. Celma, J. García del Pozo, and N. Medrano, "Fast-response low-ripple envelope follower," *Integration*, vol. 42, no. 2, pp. 169–174, 2009.

[2] S. Bhattacharyya and D. W. Graham, "Amplitude-regulated quadrature sine-VCO employing an OTA-C topology," *IEEE Transactions on Circuits and Systems II: Express Briefs*, vol. 70, no. 6, pp. 1886–1890, 2023.

[3] R. Paley and N. Wiener, "Fourier transforms in the complex domain," *Mathematical Gazette*, vol. 19, no. 233, pp. 147–148, 1935.

[4] B. Linares-Barranco, A. Rodriguez-Vazquez, E. Sanchez-Sinencio, and J. L. Huertas, "Generation, design and tuning of OTA-C high-frequency sinusoidal oscillators," *IEE Proceedings G - Circuits, Devices and Systems*, vol. 139, no. 5, pp. 557–568, 1992.

[5] V. Totik, "Bernstein-type inequalities," *Journal of Approximation Theory*, vol. 164, no. 10, pp. 1390–1401, 2012.